Article

Polymeric Coatings for Skutterudite-Based Thermoelectric Materials

Witold Brostow [1,2,*], **IKang Chen** [1,2] **and Haley E. Hagg Lobland** [1,2]

1   Laboratory of Advanced Polymers and Optimized Materials (LAPOM), Department of Materials Science and Engineering, University of North Texas, 3940 North Elm Street, Denton, TX 76207, USA; luke020519@yahoo.com (I.C.); haleylobland@gmail.com (H.E.H.L.)
2   Department of Physics, University of North Texas, 3940 North Elm Street, Denton, TX 76207, USA
*   Correspondence: wkbrostow@gmail.com

Abstract: Thermoelectric (TE) devices have short service lives. These materials undergo thermal degradation at elevated temperatures by processes such as oxidation or sublimation. Our substrates were skutterudite-based TE materials. We covered their surfaces with a liquid high-temperature polymer (HTP)—crosslinked after the deposition, what converted those surfaces into solid coatings. Sintering was performed at 250 °C for times of up to 48 h on both uncoated (control) and HTP-coated samples. The changes caused by thermal degradation were evaluated by thermogravimetric analysis, electrical resistivity, and energy-dispersive X-ray spectroscopy, and observed by scanning electron microscopy. Significant mitigation of oxidation and sublimation of our TE materials was achieved.

Keywords: thermoelectric devices; polymer crosslinking; polymeric coatings; thermal degradation; skutterudites

1. Introduction

Thermoelectric (TE) devices contain TE materials. *TE coolers* create a temperature difference ΔT when a current flows through the device. This is a manifestation of the Peltier effect—so named after a French physicist, Jean Peltier, who worked in Paris. There is also a twin effect, namely one can have a *TE generator*: a voltage V is created when different temperatures are applied to the two sides of the device. This is known as the Seebeck effect, so named after the Estonian−German physicist Thomas Johann Seebeck, who worked in Tallinn. Both kinds of TE devices have small size, no moving components, and work without noise [1–16]. As discussed by Abbas [16], thermoelectric materials can be classified as smart materials and be used for changing the electrical properties of nanostructures.

Given these advantages, TE devices are widely used in microelectronics, in optical components, medical equipment, biochemical or portable electronic equipment communications and when electromagnetic processing of materials is important [17]. Parashchuk and his colleagues [18] have created p-type $Bi_{0.5}Sb_{1.5}Te_3$ films on a flexible substrate with high thermoelectric performance. TE properties can be present together with magnetic ones—as in the $Bi_2Sr_2Co_{1.8}O_y$ phase created by Özçelik and coworkers [19]. Pristine Bi_2Te_3 and Bi_2Te_3/reduced graphene oxide (Bi_2Te_3 + rGO) composites show good electrochemical and thermoelectric properties at 1% rGO concentration—a result of the interaction of the grain boundary interfaces of rGO nanosheets with pristine Bi_2Te_3—as reported by Thongsamrit and coworkers [20]. There are also $CoSb_3$ skutterudites [21], used in TE devices for high energy conversion efficiency.

There are three main components which comprise a TE device. Two ceramics metalized with copper [22], an array of TE elements, and a solder that joins the device together; details are provided in a textbook [23].

However, the use of TE devices also involves disadvantages. The amount of electricity created by a TE generator is proportional to the temperature difference ΔT, hence one maximizes that difference as much as possible. The most often used TE material is bismuth

telluride Bi_2Te_3 [4,10,24]. At elevated temperatures, bismuth undergoes oxidation; the oxide is not thermoelectric. At elevated temperatures tellurium also escapes by sublimation. These issues are discussed below in relationship to Figure 1. Corrosion is also possible in certain environments. Our way of dealing with these problems has been covering the TE materials or entire devices with high-temperature polymers (HTPs) [25]. One has to be careful since there are polymeric nanofibers which provide high thermal conductivity useful for us—but at the same time high electric conductivity [26], which would be detrimental for us. The use of HTPs is not obvious since polymers are known for their *low* glass transition and melting temperatures; very widely used polyethylene has the melting temperature of 135 °C. However, polymers have been used in abrasion-resistant coatings for steels [27] and in corrosion-resistant coatings for Cu-Ni alloys [28]. Moreover, we have HTPs at our disposal. Sufficient protection of bismuth telluride-based up to and including 250 °C was achieved [24]. Since one typically begins with a liquid HTP—a lubricant which undergoes curing—we have studied somewhat more in detail properties of the HTP coatings, including their rheological behavior in the molten state [29].
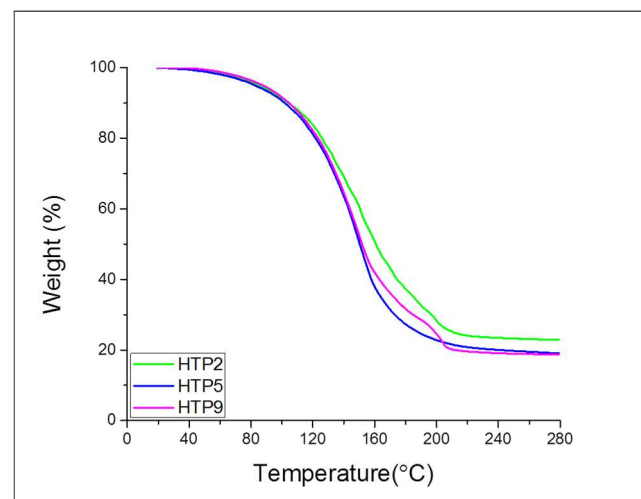

Figure 1. TGA thermograms: weight loss percentage of HTP samples treated at up to 280 °C.

Now, bismuth telluride is not the only TE material in wide use. Skutterudites are also important [30]. They contain ytterbium and antimony. In this situation, we have performed testing of skutterudite TE materials covered with an HTP with the objective of extending the service life of this class of materials.

2. Experimental

2.1. Materials

A fine-grained skutterudite micro-alloyed material (MAM) from Furukawa Co., Ltd. (Tokyo, Japan), and samples diced to needed dimensions from 3 mm × 3 mm × 5 mm cuboids were used for testing.

Three HTPs were prepared at the Laboratory of Advanced Polymers & Optimized Materials (LAPOM). HTP2 is made from a solution of an advanced polyimide. The solution is deposited on the surface as usually lubricants are so deposited, then heated to high temperature to vaporize the solvent, to accelerate the imidization reaction and make a non-soluble, non-melting insulating material with good heat resistance, chemical resistance, and providing insulation. HTP5 and HTP9 are also advanced polymeric acids with properties similar to HTP2.

2.2. Encapsulation of Skutterudite Materials

The dip coating was used to prepare TE materials. The coatings were dried and cured at elevated temperatures. Before further tests, the coatings on some skutterudite materials were removed so as to have 'naked' samples for comparison.

2.3. Thermogravimetric Analysis

The Perkin Elmer (Waltham, MA, USA) TG7 apparatus was used to perform thermal stability testing. This technique is well described by Menard and Menard [31], by Lucas and her colleagues [32], and by Gedde and Hedenqvist [33]. Seven to 10 milligrams of each HTP were heated from 50 °C to 280 °C at 10 °C/min.

2.4. Electrical Resistivity

The four-point Jandel (Leighton Buzzard, UK) RM3000 resistivity meter was used to measure electrical resistivity. The probes contacted four side surfaces of a cuboid, applied at several locations, and then averages were calculated.

2.5. Scanning Electron Microscopy and Energy-Dispersive Spectroscopy

Scanning electron microscopy (SEM) and energy-dispersive X-ray spectroscopy (EDS) of the samples was collected using a Hitachi (Tokyo, Japan) TM 3030Plus Tabletop Microscope configured with EDS.

3. Thermal Stability of HTPs

To optimize the curing process of polymeric coatings so as to achieve the highest level of protection from degradation of TE devices, we used thermogravimetric analysis (TGA) to locate temperatures of various decomposition processes. There are many factors which could affect the thermal stability of HTPs, such as pre-sintering time, temperature ramp, post-sintering time, and sintering temperature. Figure 1 shows TGA thermograms for three HTPs.

Apparently the sintering temperature is important for thermal stability of HTPs. Figure 1 tells us also that the solvents evaporated at under 200 °C. All HTPs preserved their thermal stabilities after temperature reached 220 °C to 280 °C.

4. Electrical Resistivity

After developing the optimal curing procedures for HTPs [20], we encapsulated both p-type and n-type skutterudite-based samples and subjected them to sintering up to 250 °C. The samples were ramped up to 250 °C at 1 °C/min and kept for up to 48 h at 250 °C. The bulk resistivity was determined at 25 °C for each sample. The results are shown in Figure 2 for HTP2 coatings.
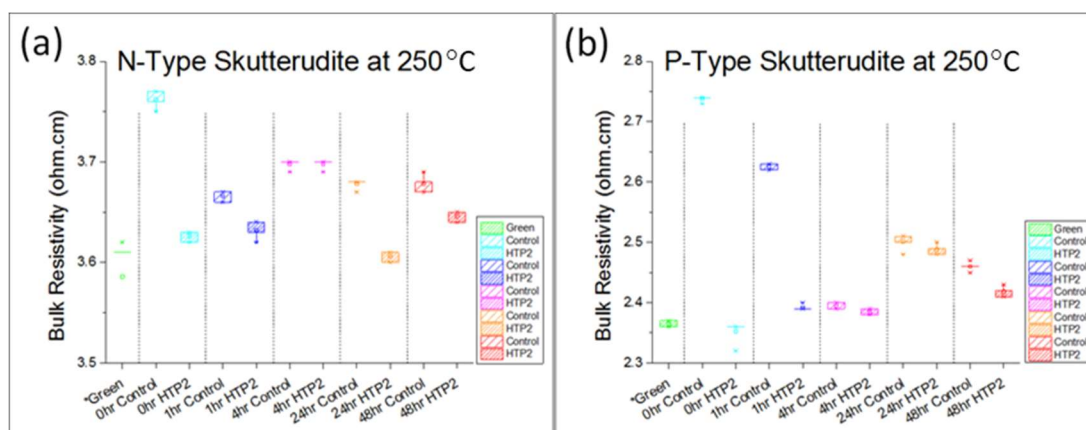

Figure 2. Bulk resistivity of skutterudite at 250 °C: (**a**) n-type; (**b**) p-type.

Due to oxidation during the sintering process, the resistivity values increased with longer sintering time in control samples (uncoated) for both p-type and n-type skutterudite-based samples. Compared with control samples at different sintering times, coatings mitigated the resistivity changes in any condition. There is a significant effect for n-type skutterudite after 24 h.

5. Sublimation and Oxidation

We have applied EDS to determine the sublimation and oxidation for both n-type and p-type skutterudite materials at different sintering times. The results are shown in Figures 3–6 and also digitized as Figures 7 and 8.
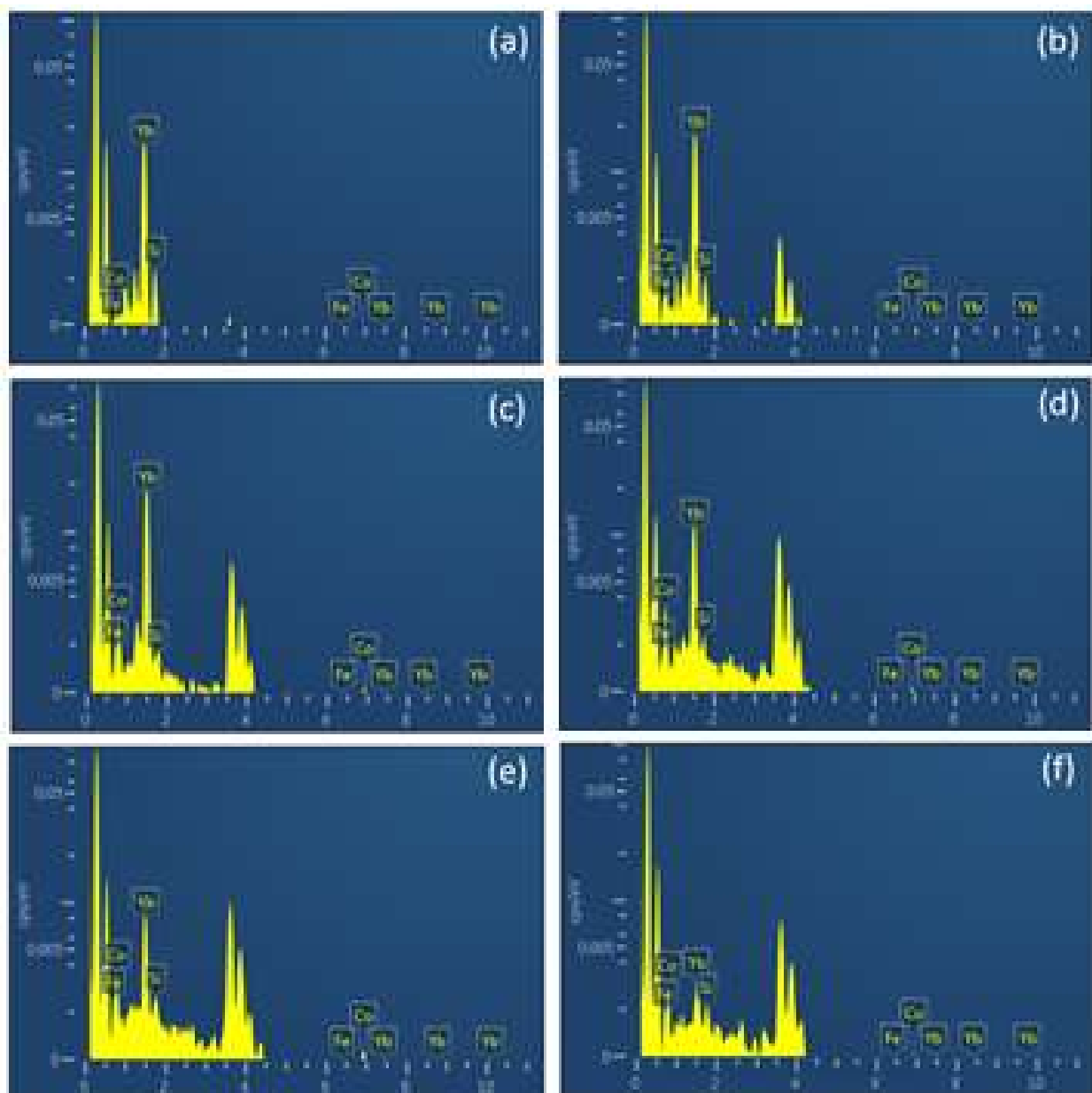

Figure 3. EDS n-type samples with HTP2 coatings: (**a**) uncoated sample at 25 °C; (**b**) sample not subjected to sintering; (**c**) sample subjected to sintering for 1 h at 250 °C; (**d**) 4 h at 250 °C; (**e**) 24 h at 250 °C; (**f**) 48 h at 250 °C.
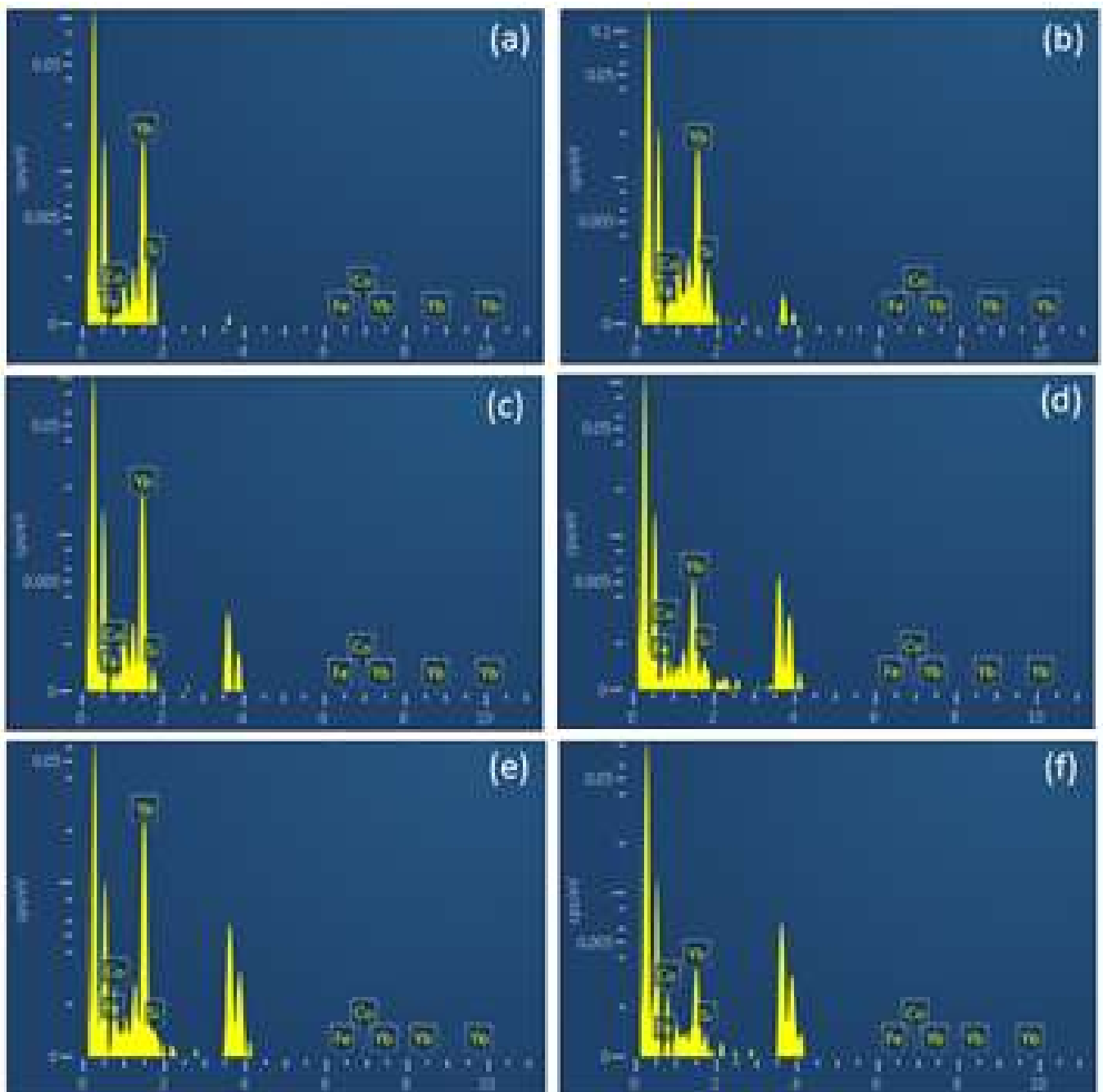
Figure 4. EDS n-type of HTP2 coated samples, some subjected to sintering at 250 °C at different sintering times: (**a**) uncoated sample not subjected to sintering; (**b**) coated sample not subjected to sintering; (**c**) sample after sintering for 1 h; (**d**) sintering for 4 h; (**e**) sintering for 24 h; (**f**) sintering for 48 h.
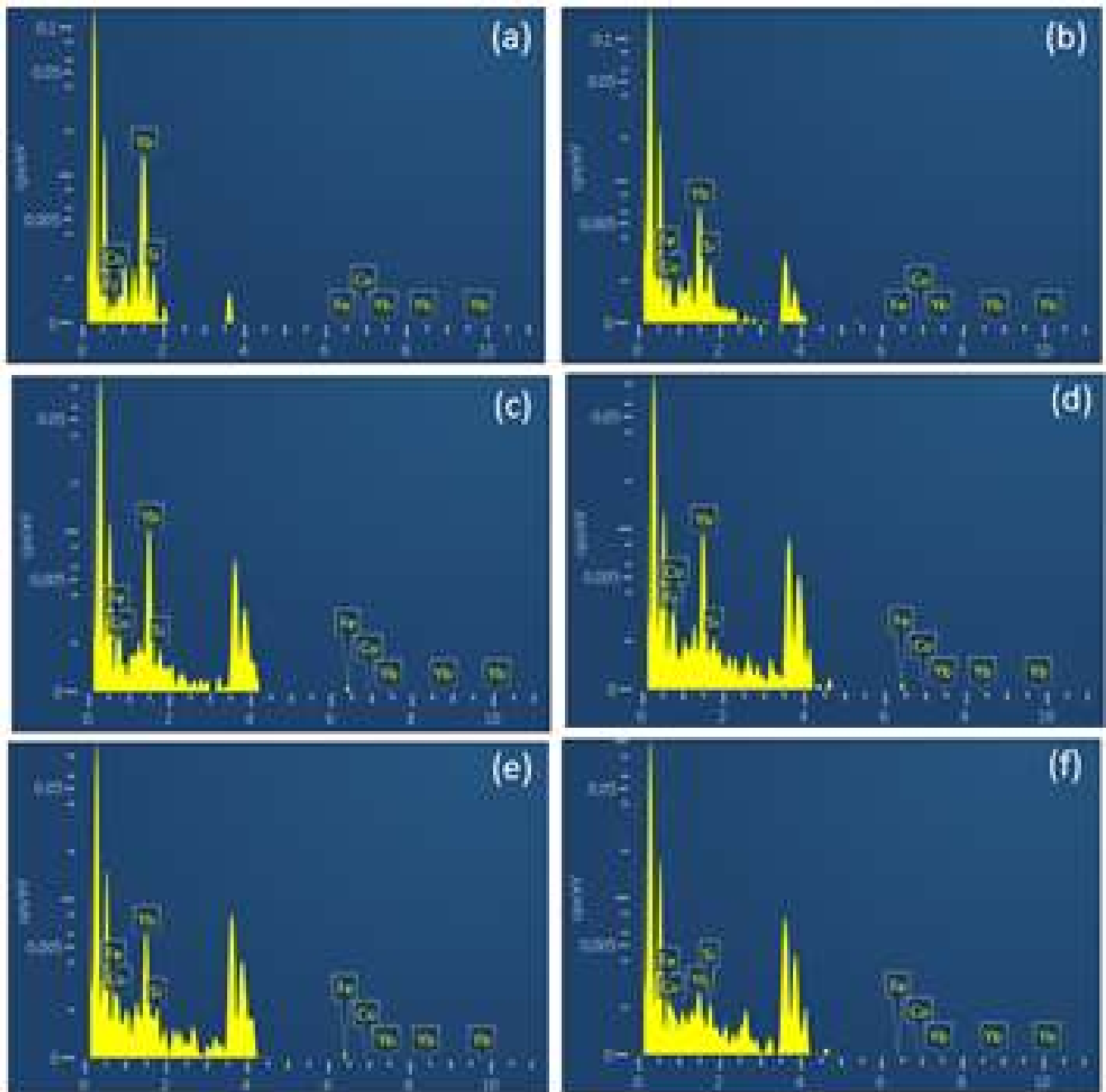
Figure 5. EDS p-type samples, most subjected to sintering at 250 °C for different sintering times: (**a**) uncoated sample at 25 °C; (**b**) coated sample not subjected to sintering; (**c**) sample after sintering for 1 h; (**d**) sintering for 4 h; (**e**) sintering for 24 h; (**f**) sintering for 48 h.

We see that both n-type and p-type samples without polymeric coatings have higher levels of sublimation. For example, ytterbium in p-type coated samples has 7 to 12% lower weight loss than uncoated samples.

We also see that the polymeric coatings are preventing the oxidation. For p-type uncoated skutterudite material with antimony which underwent longer sintering, the level of oxidation was 10% higher than for coated samples.
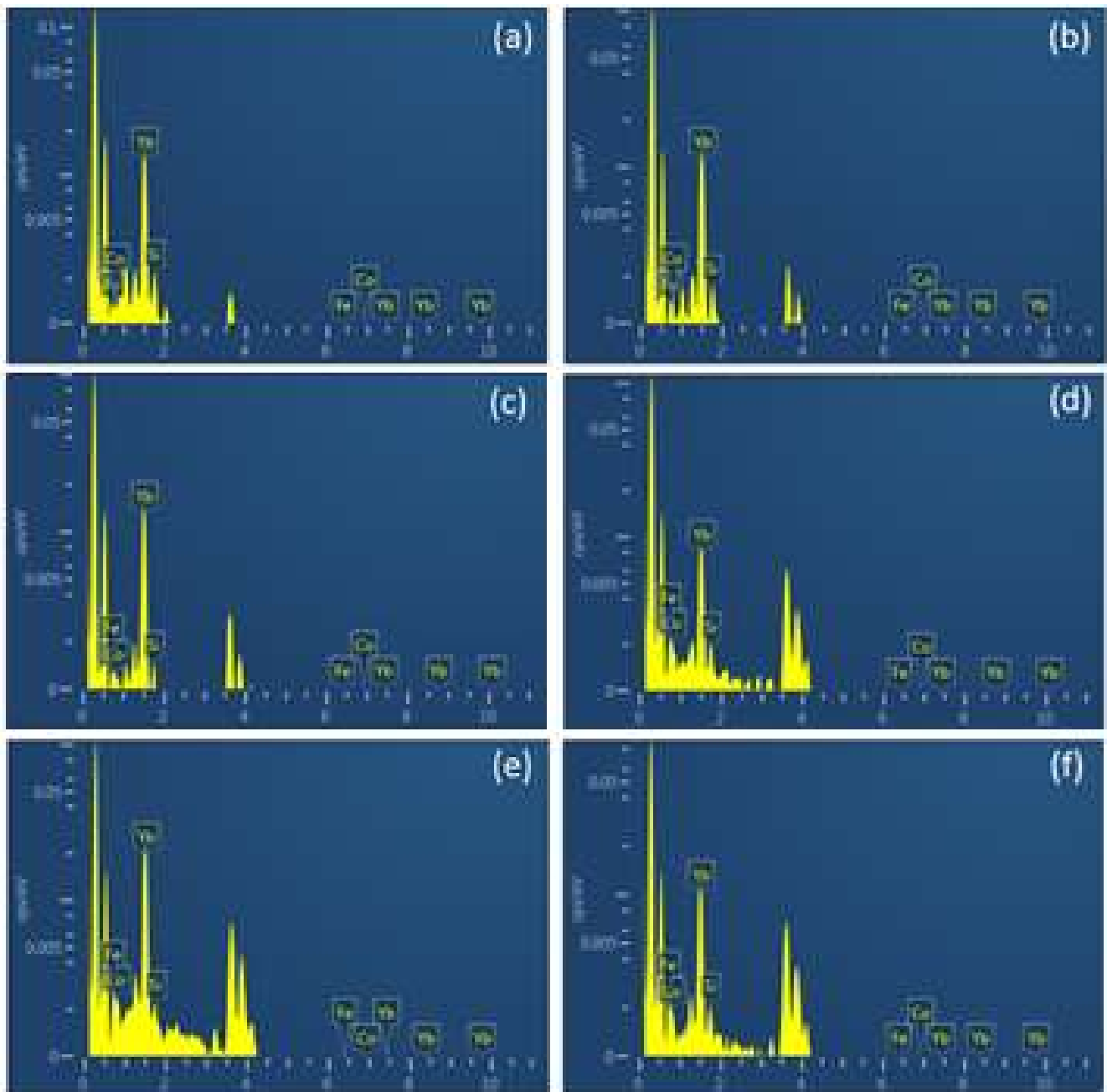
Figure 6. EDS p-type HTP2 coated samples, most sintered at 250 °C for different amounts of time: (**a**) uncoated sample at 25 °C; (**b**) coated sample, 0 h sintering; (**c**) 1 h sintering (**d**); 4 h sintering; (**e**) 24 h sintering; (**f**) 48 h sintering.
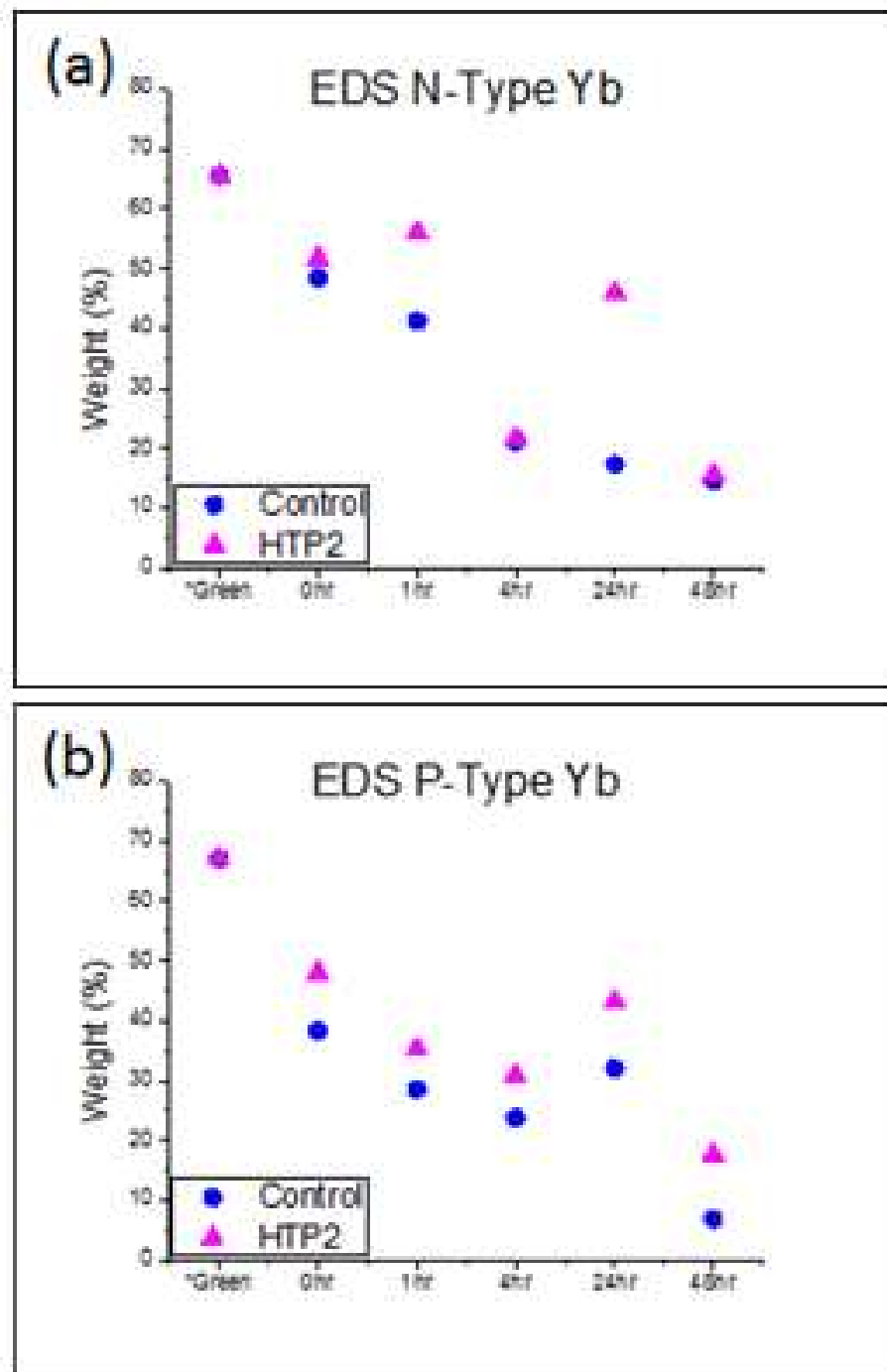
Figure 7. EDS sublimation of ytterbium: (**a**) n-type; (**b**) p-type.
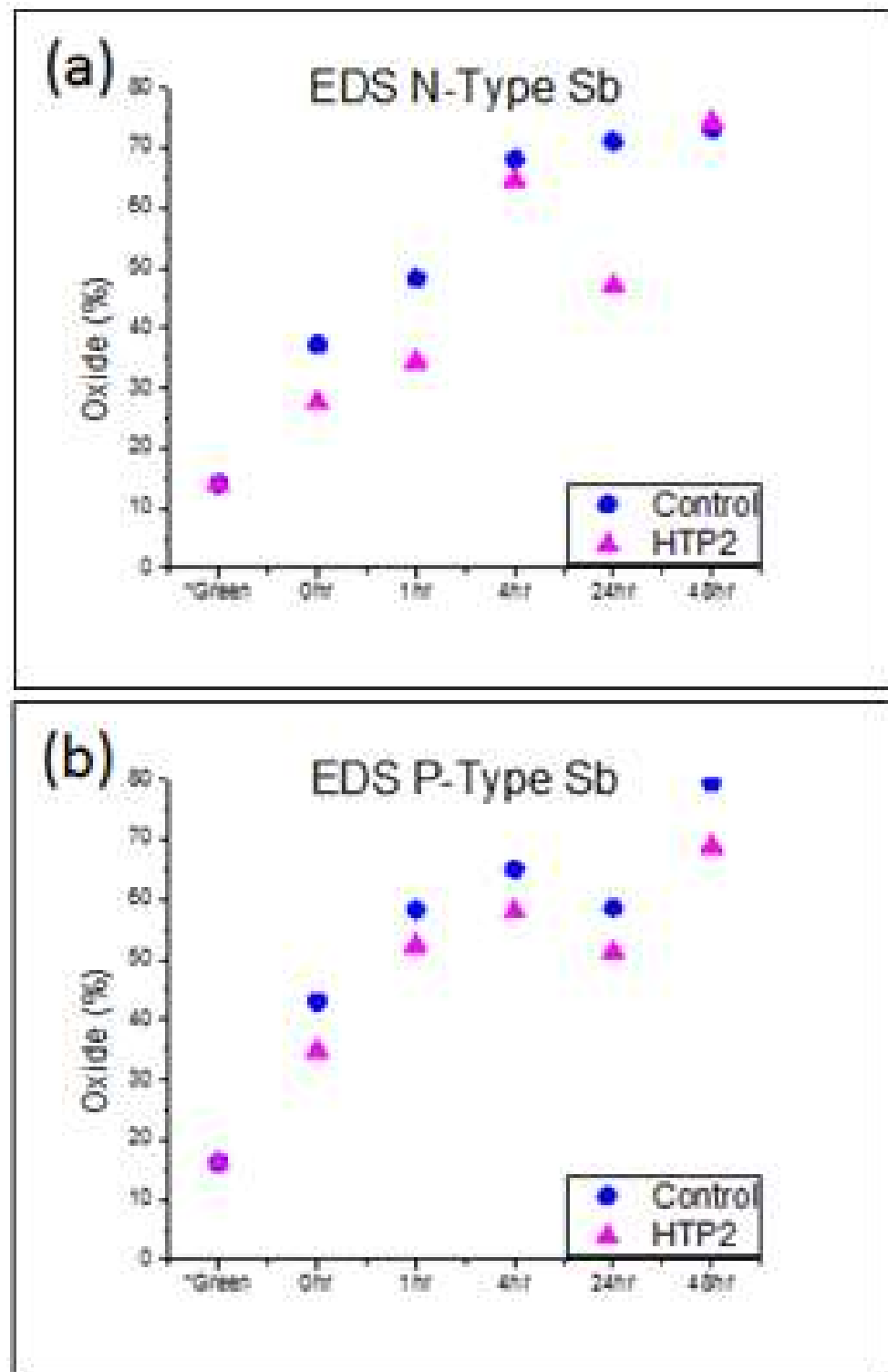
Figure 8. EDS oxidation of antimony: (**a**) n-type; (**b**) p-type.

6. Effects of Heating on Morphology

We have studied morphology of samples using environmental scanning electron microscopy (ESEM) to see visual changes—if any—during sintering. The micrographs are shown in Figures 9 and 10.
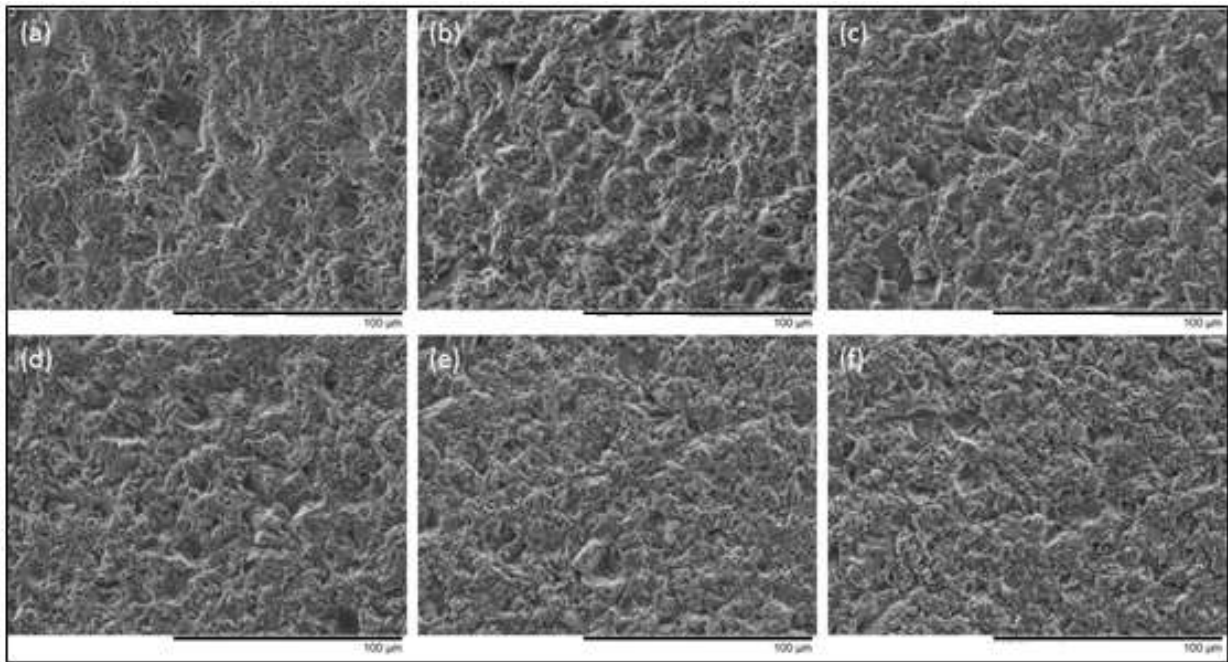
Figure 9. SEM micrographs of n-type skutterudite at different sintering conditions at 250 °C: (**a**) uncoated sample kept at 25 °C; (**b**) coated sample, 0 h sintering time; (**c**) 1 h sintering; (**d**) 4 h sintering; (**e**) 24 h sintering; (**f**) 48 h sintering.
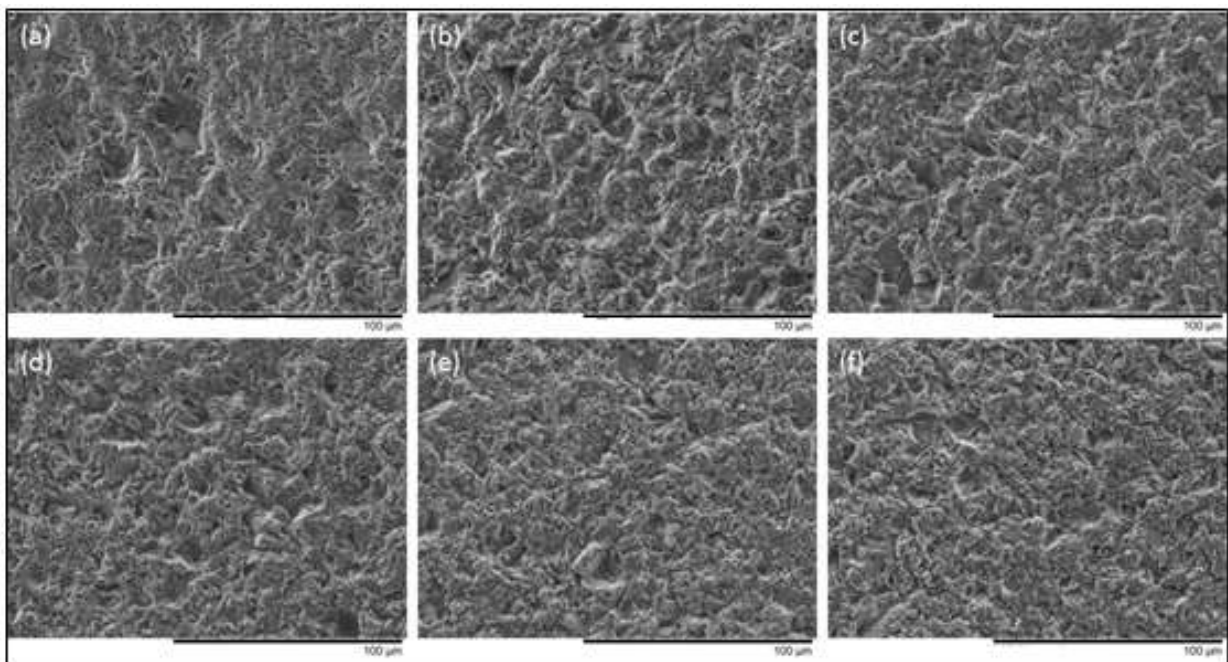

Figure 10. SEM micrographs of p-type coated skutterudite at different sintering conditions at 250 °C: (**a**) uncoated sample kept at 25 °C; (**b**) coated sample, 0 h sintering; (**c**) coated, 1 h sintering; (**d**) coated, 4 h sintering; (**e**) coated, 24 h sintering; (**f**) coated, 48 h sintering.

We do not see significant differences between Figures 9 and 10. In samples with coatings, some residues start to show up with increasing sTintering time.

7. Concluding Remarks

Our main objective was mitigation of thermal degradation of skutterudite-based thermoelectric materials—so as to extend the service life of those materials and make them more attractive for industry from the economical perspective. We had already developed improved coating and curing processes of HTPs [24]. Now we have achieved mitigation of oxidation and sublimation of skutterudite-based materials—as seen in electrical resistivity, EDS, and in SEM analysis.

Author Contributions: Data curation, W.B., I.C., and H.E.H.L.; methodology, W.B.; project administration, W.B. All authors have read and agreed to the published version of the manuscript.

Conflicts of Interest: The authors declare no conflict of interest.

References

1. DiSalvo, F.J. Thermoelectric Cooling and Power Generation. *Science* **1999**, *285*, 703–706. [CrossRef] [PubMed]
2. Kim, I.-H. (Bi,Sb)2(Te,Se)3-based thin film thermoelectric generators. *Mater. Lett.* **2000**, *43*, 221–224. [CrossRef]
3. Nolas, G.S.; Sharp, J.; Goldsmid, H.J. *Thermoelectrics Basic Principles and New Materials Developments*; Springer Series in Materials Science; Springer: Heidelberg, Germany, 2001; p. 45.
4. Beyer, H.; Nurnus, J.; Böttner, H.; Lambrecht, A.; Wagner, E.; Bauer, G. High thermoelectric figure of merit ZT in PbTe and Bi2Te3-based superlattices by a reduction of the thermal conductivity. *Phys. E Low-Dimens. Syst. Nanostructures* **2002**, *13*, 965–968. [CrossRef]
5. Riffat, S.; Ma, X. Thermoelectrics: A review of present and potential applications. *Appl. Therm. Eng.* **2003**, *23*, 913–935. [CrossRef]
6. Shikano, M.; Funahashi, R.; Kitawaki, M. Properties of CaxCo2O4 Aligned Crystals. *J. Mater. Res.* **2005**, *20*, 3082–3087. [CrossRef]
7. Rowe, D.M. *Thermoelectrics Handbook—Macro to Nano*; Taylor and Francis: New York, NY, USA, 2006.
8. Bell, L.E. Cooling, Heating, Generating Power, and Recovering Waste Heat with Thermoelectric Systems. *Science* **2008**, *321*, 1457–1461. [CrossRef]
9. Wang, L.; Wang, D.; Zhu, G.; Li, J.; Pan, F. Thermoelectric properties of conducting polyaniline/graphite composites. *Mater. Lett.* **2011**, *65*, 1086–1088. [CrossRef]
10. Goldsmid, H.J. Bismuth Telluride and Its Alloys as Materials for Thermoelectric Generation. *Materials* **2014**, *7*, 2577–2592. [CrossRef]
11. Brostow, W.; Granowski, G.; Hnatchuk, N.; Sharp, J.; White, J.B. Thermoelectric phenomena. *J. Mater. Ed.* **2014**, *36*, 175–185.
12. El-Desouky, A.; Carter, M.; Andre, M.A.; Bardet, P.M.; LeBlanc, S. Rapid processing and assembly of semiconductor thermoelectric materials for energy conversion devices. *Mater. Lett.* **2016**, *185*, 598–602. [CrossRef]
13. Brostow, W.; Sayana, S.; Sharp, J.; Thompson, A.J.; White, J.B. Thermoelectric materials. *J. Mater. Ed.* **2017**, *39*, 259–269.
14. Kim, J.; Duy, L.T.; Kang, H.; Ahn, B.; Seo, H. Fluorine doping for improved thermoelectric properties of spark plasma sintered bismuth telluride. *J. Mater. Sci. Technol.* **2021**, *90*, 225–235. [CrossRef]
15. Kim, S.-T.; Park, J.M.; Park, K.-I.; Chun, S.-E.; Lee, H.S.; Choi, P.-P.; Yi, S. Enhanced thermoelectric composite performance from mesoporous carbon additives in a commercial Bi0.5Sb1.5Te3 matrix. *J. Mater. Sci. Technol.* **2021**, *94*, 175–182. [CrossRef]
16. Abbas, M. Smart materials for changing the electrical properties of nanostructures. *Compos. Adv. Mater.* **2021**, *30*, 1–16. [CrossRef]
17. Biesuz, M.; Saunders, T.; Ke, D.; Reece, M.J.; Hu, C.; Grasso, S. A review of electromagnetic processing of materials (EPM): Heating, sintering, joining and forming. *J. Mater. Sci. Technol.* **2021**, *69*, 239–272. [CrossRef]
18. Parashchuk, T.; Kostyuk, O.; Nykyruy, L.; Dashevsky, Z. High thermoelectric performance of p-type Bi0.5Sb1.5Te3 films on flexible substrate. *Mater. Chem. Phys.* **2020**, *253*, 123427. [CrossRef]
19. Özçelik, B.; Çetin, G.; Gürsul, M.; Madre, M.; Sotelo, A. A study on thermoelectric performance and magnetic properties of Ti-doped Bi2Sr2Co1.8Oy ceramic materials. *Mater. Chem. Phys.* **2020**, *256*, 123701. [CrossRef]
20. Thongsamrit, W.; Promphet, C.; Maneesai, K.; Karaphun, A.; Tuichai, W.; Sriwong, C.; Ruttanapun, C. Effect of grain boundary interfaces on electrochemical and thermoelectric properties of a Bi2Te3/reduced graphene oxide composites. *Mater. Chem. Phys.* **2020**, *250*, 123196. [CrossRef]
21. Zheng, Z.-H.; Shi, X.-L.; Ao, D.-W.; Liu, W.-D.; Chen, Y.-X.; Li, F.; Chen, S.; Tian, X.-Q.; Li, X.-R.; Duan, J.-Y.; et al. Rational band engineering and structural manipulations inducing high thermoelectric performance in n-type CoSb3 thin films. *Nano Energy* **2020**, *81*, 105683. [CrossRef]
22. Brostow, W.; Datashvili, T.; McCarty, R.; White, J.B. Copper viscoelasticity manifested in scratch recovery. *Mater. Chem. Phys.* **2010**, *124*, 371–376. [CrossRef]

23. Brostow, W.; Hagg Lobland, H.E. *Materials: Introduction and Applications*; John Wiley & Sons: Hoboken, NJ, USA, 2017.
24. Brostow, W.; Chen, I.K.; White, J.B. Effects of polymeric coatings on the service life of bismuth telluride-based thermoelectric materials. *Sustain. Energy Fuels* **2017**, *1*, 1376–1380. [CrossRef]
25. Brostow, W.; Datashvili, T.; Lobland, H.E.H.; Hilbig, T.; Su, L.; Vinado, C.; White, J. Bismuth telluride thermoelectric materials: Coatings as protection against thermal cycling effects. *J. Mater. Res.* **2012**, *27*, 2930–2936. [CrossRef]
26. Arenas, M.C.; Andablo, E.; Castaño, V.M. Synthesis of conducting polyaniline nanofibers from single and binary dopant agents. *J. Nanosci. Nanotechnol.* **2010**, *10*, 549–554. [CrossRef] [PubMed]
27. Vijay, P.V.; Soti, P.R.; Banerjee, D.A.; Sierros, K.A. Abrasion resistance of polymer and polymer–ceramic composite coatings for steel hydraulic structures. *J. Coatings Technol. Res.* **2020**, *17*, 401–411. [CrossRef]
28. Jena, G.; Vanithakumari, C.; Polaki, S.R.; George, R.P.; Philip, J.; Amarendra, G. Electrophoretically deposited graphene oxide–polymer bilayer coating on Cu-Ni alloy with enhanced corrosion resistance in simulated chloride environment. *J. Coatings Technol. Res.* **2019**, *16*, 1317–1335. [CrossRef]
29. Brostow, W.; Chang, J.; Lobland, H.E.H.; Perez, J.M.; Shipley, S.; Wahrmund, J.; White, J.B. Rheological Characterization of Liquid Polymers Containing Ceramic Nanopowders for Use in Thermoelectric Devices. *J. Nanosci. Nanotechnol.* **2015**, *15*, 6604–6608. [CrossRef]
30. Nolas, G.; Fowler, G. Partial filling of skutterudites: Optimization for thermoelectric applications. *J. Mater. Res.* **2005**, *20*, 3234–3237. [CrossRef]
31. Menard, K.P.; Menard, N.R. *Dynamic Mechanical Analysis*, 3rd ed.; CRC Press: Boca Raton, FL, USA, 2020.
32. Lucas, E.F.; Soarez, B.G.; Monteiro, E. *Caracterização de Polimeros*; E-Papers: Rio de Janeiro, Brazil, 2001.
33. Gedde, U.W.; Hedenqvist, M.S. *Polymer Physics*, 2nd ed.; Springer Nature Switzerland AG: Cham, Switzerland, 2019.